Materials Science-Poland, Vol. 24, No. 3, 2006

Magnetisation and electron spin resonance of the colossal magnetoresistive $La_{0.67}Ca_{0.33}Mn_{1-x}Fe_xO_3$

T. ZAJĄC[1], L. FOLCIK[2], J. CHMIST[1], A. KOŁODZIEJCZYK[1*],
H. DRULIS[2], K. KROP[1], G. GRITZNER[3]

[1]Faculty of Physics and Applied Computer Science, AGH University of Science and Technology,
30-059 Cracow, Poland

[2]Institute of Low Temperature and Structure Research, Polish Academy of Sciences,
50-950 Wrocław, Poland

[3]Institut für Chemische Technologie Anorganischer Stoffe, Johannes Kepler Universität,
A-4040 Linz, Austria

We report magnetisation and electron spin resonance (ESR) measurements on the colossal magnetoresistive manganites $La_{0.67}Ca_{0.33}Mn_{1-x}Fe_xO_3$, with $x = 0$, 0.01, 0.03, 0.06, 0.10, and 0.15, in the vicinity of their magnetic (T_C) and metal-insulator (T_{MI}) transition temperatures. Above T_C, the resonance lines with $g \approx 2$ are caused by ferromagnetic metallic clusters exhibiting a double exchange interaction between Mn^{3+}–Mn^{4+} ions. The lines were observed with cooling far below both T_C and T_{MI}, and were fitted by the Dysonian line-shape. The temperature dependences of the line-widths exhibited a minimum value at $T_{\min} \approx 1.25T_C$, followed by an increase with further cooling toward T_C. The anomalous behaviour of the line-width below $T_{\min}$ is due to the appearance of a ferromagnetic metallic phase within the paramagnetic matrix. The role of phase segregation, in which the compounds are phase-separated into a mixture of ferromagnetic and paramagnetic regions, is discussed.

Key words: *iron substituted manganite; electron spin resonance; ESR; phase segregation*

1. Introduction

The system $Ln_{2/3}B_{1/3}MnO_3$, where Ln is a rare earth ion and B a divalent alkali metal, has been the most widely studied among all ABO_3-type perovskite manganites [1]. In the manganites, the doping concentration introduces a mixed valence (Mn^{3+}, Mn^{4+}), which governs the magnetic and electric properties of the compounds. The system undergoes a transition from a paramagnetic insulating (PMI) to a ferromagnetic metallic (FMM) state when temperature is decreased. Around that transition,

---

[*] Corresponding author, e-mail: akolo@uci.agh.edu.pl

a resistance maximum is observed, which is largely suppressed by magnetic field, leading to an observation of the colossal magnetoresistance effect (CMR). The metal-to-insulator transition temperature T_{MI} is sometimes significantly different from the Curie temperature T_C. Various mechanisms have been proposed to explain the CMR effect, nonetheless the physical origin of the transition is still a matter of controversy [1–3]. Most frequently, the Zener double-exchange model (DE) [4] is proposed to understand the magnetic and electrical properties of the materials. Electronic phase separation into conducting ferromagnetic clusters, coupled via DE interaction between Mn^{3+} and Mn^{4+} ions with a characteristic lifetime τ exceeding 10^{-5} s [5], has recently been considered responsible for their CMR.

We have performed ESR studies on iron-substituted manganites to search for the dynamic properties of the mechanism of double exchange interaction between itinerant e_g electrons and localised t_{2g} electrons forming the $S = 3/2$ spins of Mn^{4+} ions. The magnetic moments of these clusters and their concentrations are responsible for the ESR signal.

2. Experimental results and analysis

Polycrystalline samples of $La_{0.67}Ca_{0.33}Mn_{1-x}Fe_xO_{3+\delta}$, with $x = 0$, 0.01, 0.03, 0.06, 0.10, and 0.15, were prepared by the wet sol-gel method and solid-state reaction with $\delta \approx 0$, which were performed by the same procedure as in [6]. The overall stoichiometry was determined by a thermogravimetric method. The crystal structure and exact stoichiometry were determined from precise the X-ray diffraction by a Siemens 5050 diffractometer, using the Rietveld procedure and Full-prof fitting programme. The lattice parameters were calculated from the XRD data. Each of the investigated compounds was found to consist of a single phase.

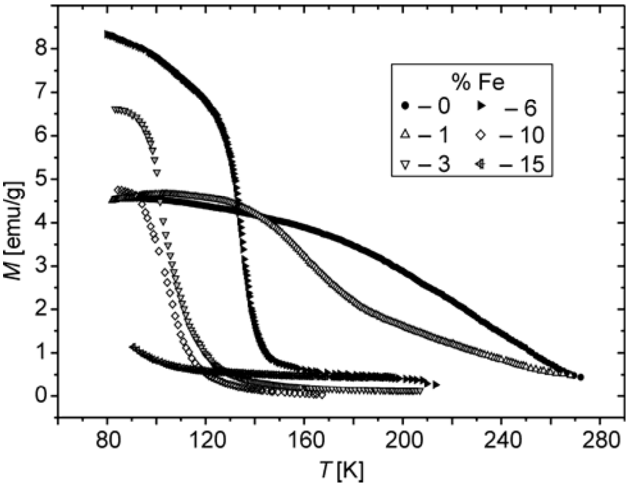

Fig. 1. Temperature dependence of magnetisation for $La_{0.67}Ca_{0.33}Mn_{1-x}Fe_xO_3$ with a given x in a magnetic field of 100 Oe

The susceptibilities and specific heats of some of the compounds have been described previously [7]. Specifically, for the present study all samples were magnetically characterized with the help of a standard vibrating sample magnetometer (VSM), in a magnetic field of 100 Oe, and as a function of temperature from 77 K up to room temperature (Fig. 1). DC magnetization was recorded during heating in the applied DC field after zero-field cooling (ZFC) down to 77 K. Magnetisation was measured for powdered specimens.

Curie temperatures were determined from the temperature dependence of magnetisation as the inflection point of the $M(T)$ curve at 100 Oe (Fig. 1), i.e. the temperature corresponding to the minimum of the dM/dT curve. T_C decreases from 262 K for $x = 0$, through 166 K for $x = 0.01$, 102 K for $x = 0.03$, 126 K for $x = 0.06$, and to 104 K for $x = 0.1$. The error of T_C is about 2 K. The Curie temperature $T_C \approx 80\pm5$ K for $x = 0.15$ was estimated from extrapolation of the experimental points in Fig. 1 to lower temperatures by a fifth order polynomial fit followed by differentiation. ESR spectra were carried out at X-band microwave radiation ($\nu = 9.5$ GHz) in the temperature range 4.2–300 K in magnetic fields up to 0.7 T by a microwave spectrometer equipped with a continuous gas-flow cryostat for He (Oxford Instruments). Bulk or powder samples were placed into quartz tubes in the cylindrical resonant cavity. Selected spectra are shown in Figs. 2 and 3 as examples.

From the spectra in Fig. 2 for the sample with $x = 0$, the single asymmetric, rather narrow line in the paramagnetic region above T_C undergoes a transition to the very broad single line in the low-temperature ferromagnetic region. The same behaviour is observed in Fig. 3 for the sample with $x = 0.1$, but the paramagnetic line exists far below the paramagnetic-ferromagnetic transition at T_C. In the intermediate region around the magnetic phase transition, both lines are visible. These are characteristic observations of all investigated samples. In our previous paper [8], more spectra were presented. Therein, the qualitative analysis of these spectra was restricted to ESR above the Curie temperature T_C.

In the frame of the present paper, quantitative analysis of ESR spectra above and below T_C was performed in according to the approach presented previously [9, 10]. As one can see from Figs. 2 and 3, far below T_C a very broad ferromagnetic resonant line (FMR) was detected in addition to the ESR line. The FMR line gradually disappears below T_C, because when temperature is decreased the sample enters the unsaturated magnetisation state at the given applied magnetic fields and the resonant condition is not further fulfilled. We leave the analysis of the FMR lines for future studies. Here, our analysis is restricted to the ESR lines above and below T_C. It has already been established [8–11] that the ESR lines come from ferromagnetic and metallic clusters of Mn^{3+}–Mn^{4+} ions coupled via double exchange interactions. These clusters are embedded in a paramagnetic matrix above T_C and in a ferromagnetic matrix below T_C due to the phase-separation phenomenon [5, 8–11].

The single, rather broad asymmetric lines detected in the paramagnetic region (see Figs. 2 and 3) are usually fitted with the Dysonian line shape [8–12]. From the first derivative of the microwave absorbed power P with respect to the applied magnetic field B, the line-widths ΔB and resonance fields B_{res} were derived by fitting with a proper combination of absorptive and dispersive Lorentzian terms, following the method proposed in [12]:

$$\frac{dP}{dB} \propto \frac{d}{dB}\left(\frac{\Delta B + \alpha\left(B - B_{\mathrm{res}}\right)}{\left(B - B_{\mathrm{res}}\right)^2 + \Delta B^2} + \frac{\Delta B + \alpha\left(B - B_{\mathrm{res}}\right)}{\left(B + B_{\mathrm{res}}\right)^2 + \Delta B^2}\right) \tag{1}$$

where α is the ratio of the dispersion to the absorption line components.

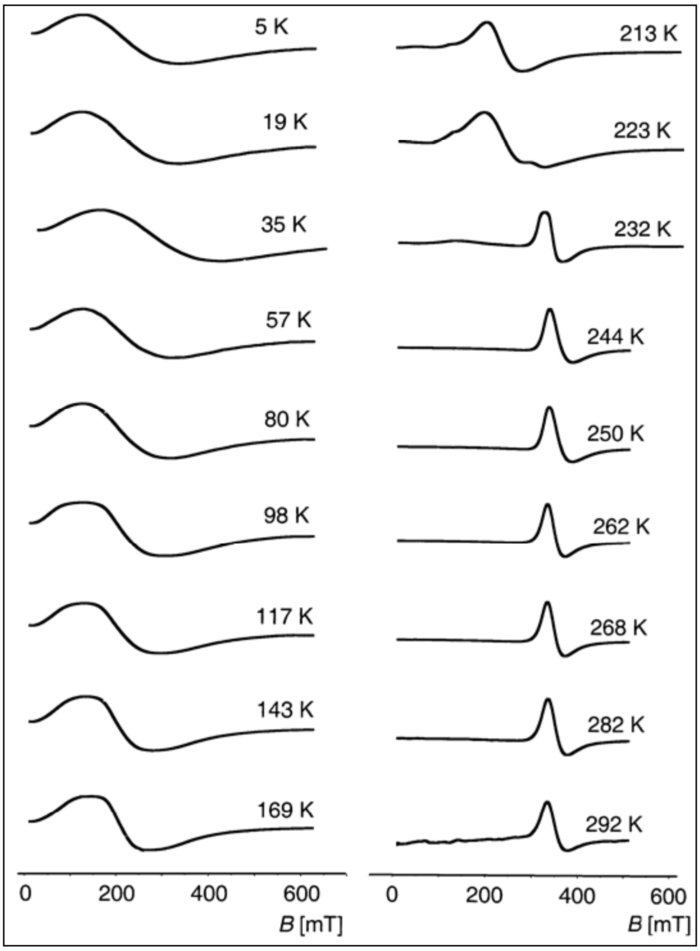

Fig. 2. Temperature dependence of the ESR spectra of $La_{0.67}Ca_{0.33}Mn_{1-x}Fe_xO_3$ for $x = 0$

The resonance field of all investigated compounds in the paramagnetic region yields the g-factor value of 1.98–2.00, slightly below the free electron value. For a single run of measurements for bulk $La_{0.67}Ca_{0.33}MnO_3$, we detected the asymmetric two-component resonant and anti-resonant structure of the line due to the sufficiently high conductivity of the compound [11]. The ratio α changes from nearly zero to about 2 as x increases, and obeys a very similar temperature dependence as the absorption line width. All recorded paramagnetic Dysonian-like shaped spectra were successfully decomposed into absorption and dispersive components. The temperature dependences of the absorption line-width are shown in Fig. 4.

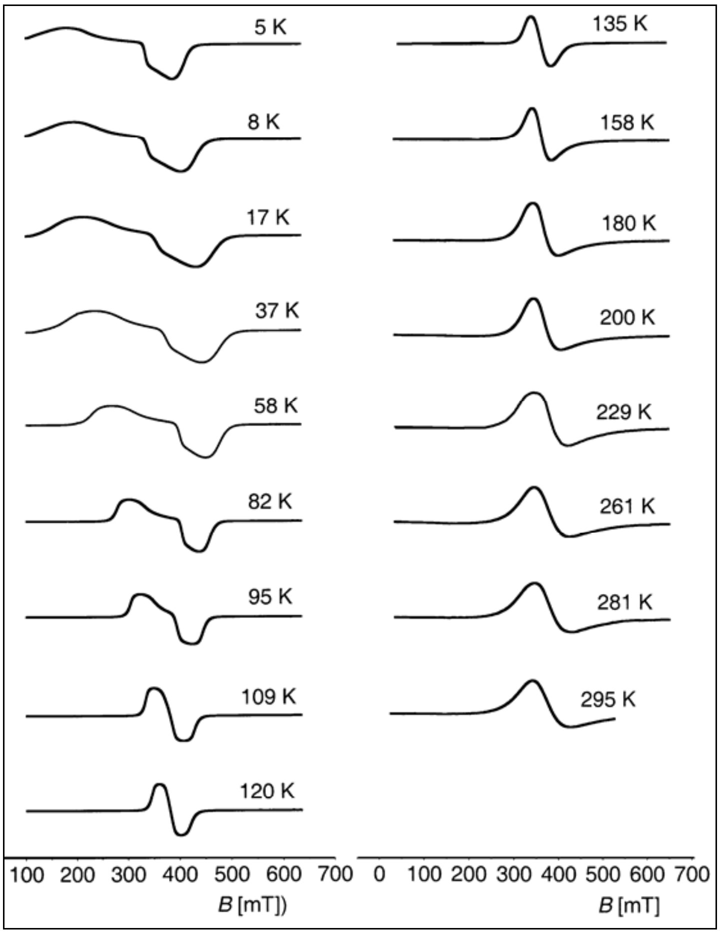

Fig. 3. Temperature dependence of the ESR spectra of $La_{0.67}Ca_{0.33}Mn_{1-x}Fe_xO_3$ for $x = 0.1$

The dependences exhibit minima at $T_{min} \approx 1.2T_C$. Above the minimum, the line-widths increase with temperature due to the spin lattice relaxation of clusters of Mn^{3+} $-Mn^{4+}$ ions coupled via double exchange interactions. We assumed that the temperature dependence of the line-width $\Delta B(T)$ above T_{min} might be described by the saturation Boltzmann curve:

$$\Delta B(T) = \Delta B_{max} + \frac{\Delta B_{min} - \Delta B_{max}}{\left(1 + e^{(T-T_0)/\delta T}\right)} \tag{2}$$

The line-width reaches a minimum $\Delta B_{\min}$ at $T_{\min}$ and a maximum $\Delta B_{\max}$ for $T \to \infty$. The function $\Delta B(T)$ possesses an inflection point at T_0. Figure 4 shows the fitting of Eq. (2) above $T_{\min}$. The values of parameters $\Delta B_{\min}$ and $\Delta B_{\max}$ are listed in Table 1.

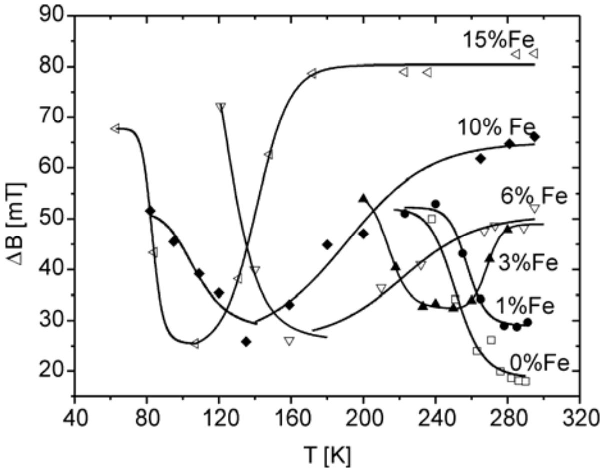

Fig. 4. Temperature dependence of the resonance line width for the indicated compounds

Table 1. Fitting parameters of the temperature dependence of resonance line widths for $La_{0.67}Ca_{0.33}Mn_{1-x}Fe_xO_3$ (shown in Fig. 4) according to Eqs (2) and (3)

x	$\Delta B_{\min}$ [mT]	ΔB [mT]	U/k_B [K]	$\Delta B_{\max}$ [mT]	T_0 [K]	δT [K]
0	18.6	33.4	8445	–	–	–
0.01	29	23.3	12860	–	–	–
0.03	32.4	22.8	8345	48.9	268	4.1
0.06	26	71.6	1910	50.6	221.6	20.4
0.10	18	34.6	1824	66.3	181	30.7
0.15	25.4	42.3	2360	80.3	140	9.3

The temperature dependence of the line width below $T_{\min}$ obeys the temperature dependence of magnetisation (Figs. 1 and 4), as well as magnetoresistance [1, 7]. In Ref. [9], it is described by the equation:

$$\Delta B(t) = \Delta B_{\min} + \frac{\Delta B_0 - \Delta B_{\min}}{1 + \mathrm{e}^{-U(1-t)/k_B T}} \tag{3}$$

where ΔB_0 is the line width at $T = 0$, $t = T/T_C$, and U is the activation energy. We followed the approach, and the fitted curves below $T_{\min}$ are shown in Fig. 4. The values of U/k_B and $\Delta B = \Delta B_0 - \Delta B_{\min}$ are listed in Table 1.

From the quantitative analysis we can conclude that the ESR line comes entirely from Mn^{3+}–Mn^{4+} clusters, because ESR measures an average state due to the jumping of electrons between these two manganese valence states. With an increasing concentration of Fe, which is in the Fe^{3+} ionic state [1], the concentration of Mn^{3+} ions decreases mainly within the clusters. Since the ESR line width increases (Fig. 4), i.e. the cluster spin-lattice relaxation time decreases with the concentration of Fe at $T \to \infty$, as well as with temperature above $T_{\min}$, we conclude that substitution by iron weakens the double exchange interaction within Mn^{3+}–Mn^{4+} clusters.

3. Conclusions

We concluded that ferromagnetic metallic clusters, exhibiting double exchange interactions between Mn^{3+}–Mn^{4+} ions, play a dominant role in resonant absorption. The temperature dependences of absorption line width exhibit a minimum value at $T_{\min} \cong 1.2T_C$ and in the region below $T_{\min}$ follow the temperature dependences of magnetisation and magnetoresistance (Eq. (3)). Above $T_{\min}$, the line width increases and reaches $\Delta B_{\max}$ at high temperatures. In this region, the temperature dependence of line width obeys the saturation curve (Eq. (2)).

Acknowledgements

This work was financially supported by the Faculty of Physics and Applied Computer Science, AGH University of Science and Technology, Cracow, Poland and by the Polish–Austria Co-operation project.

References

[1] Dagotto E., Hotta T., Moreo A., Phys. Rep., 344 (2001), 1.

[2] Yuan S.L., Li J.Q., Jiang Y., Yang Y.P., Zeng X.Y., Li G., Tu F., Zhang G.Q., Tang C.Q., Jin S.Z., Phys. Rev. B, 62 (2000), 5313.

[3] Rettori C., Rao D., Singley J., Kidwell D., Oseroff S.B., Causa M.T., Neumeier J.J., Mc Clellan K.J., Cheong S-W., S.Schultz, Phys. Rev. B 55 (1997), 3083.

[4] Zener C., Phys. Rev., 82 (1951), 403.

[5] Kapusta C., Riedi P., J. Mag. Mag. Mater., 196–197 (1999), 446.

[6] Przewoźnik J., Chmist J., Kolwicz-Chodak L., Tarnawski Z., Kołodziejczyk A., Krop K., Kellner K., Gritzner G., Acta Phys. Polon. A, 106 (2004), 665.

[7] Tarnawski Z., Waśniowska M., Chmist J., Sechovsky V., Kołodziejczyk A., Kozłowski A., Krop K., Gritzner G., Physica B, 329–333 (2003), 721.

[8] Zając T., Folcik L., Kołodziejczyk A., Drulis H., Krop K., Gritzner G., J. Mag. Mag. Mater., 272–276 (2004), 120.

[9] Yuan S.L., Zhao W.Y., Zhang G.Q., Tu F., Peng G., Liu J., Yang P.Y., Li G., Jiang Y., Zeng X.Y., Tang C.Q., Appl. Phys. Lett., 77 (2000), 4398.

[10] Li J.Q., Yuan S.L., Solid State Commun., 129 (2004), 431.

[11] de Brion S., Dupont F., Reinke D., G.Chouteau, Appl. Magn. Res., 19 (2000), 547.

[12] Peter M., Shaltiel D., Wernick J.H., Williams H.J., Mock J.B., Sherwood R.C., Phys. Rev., 126 (1962), 1395.

Received 1 June 2005
Revised 10 October 2005